Functional analysis of the human NRAMP family expressed in fission yeast

Mitsuaki TABUCHI*, Tsutomu YOSHIDA†, Kaoru TAKEGAWA‡ and Fumio KISHI*[1]

*Centre for Gene Research, Yamaguchi University, 1-1-1 Minami-Kogushi, Ube, Yamaguchi 755-8505, Japan, †Ube Research Laboratory, FUJIREBIO Inc., Ube, Yamaguchi 759-0134, Japan, and ‡Department of Life Sciences, Faculty of Agriculture, Kagawa University, Miki-cho, Kagawa 761-0795, Japan

The *Bcg/Ity/Lsh* locus in the mouse genome regulates macrophage activation for antimicrobial activity against intracellular pathogens, and the positional cloning of this locus identified the *Nramp1* (natural resistance-associated macrophage protein) gene. *Nramp2* was initially isolated as a homologue of *Nramp1*. Recently, the rat divalent metal transporter *DMT1* was identified electrophysiologically, and was found to be an isoform of *Nramp2*, a mutation which was subsequently identified in rats suffering from hereditary iron-deficiency anaemia. Despite the 64% amino acid sequence identity of Nramp1 and Nramp2, no divalent metal transport activity has yet been detected from Nramp1, and the function of Nramp1 on the molecular level is still unclear. To investigate the divalent metal transport activity of NRAMP molecules, we constructed four chimeric NRAMP genes by swapping the domains of human NRAMP1 and NRAMP2 with each other. The functional characteristics of wild-type NRAMP1, NRAMP2 and their chimeras were determined by expression in the divalent metal transporter-disrupted strain of fission yeast, *pdt1Δ*, and we analysed the divalent metal transport activity by complementation of the EGTA- and pH-sensitive phenotype of *pdt1Δ*. Replacement of the N-terminal cytoplasmic domain of NRAMP2 with the NRAMP1 counterpart resulted in inactive chimeras, indicating that the functional difference between NRAMP1 and NRAMP2 is located in this region. However, results obtained with the reverse construct and other chimeras indicated that these regions are not solely responsible for the differences in EGTA- and pH-sensitivity of NRAMP1 and NRAMP2. These findings indicate that NRAMP1 itself cannot represent the divalent metal transport activity in *S. pombe* and the additional protein segments of the molecules located elsewhere in NRAMP1 are also functionally distinct from their NRAMP2 counterparts.

Key words: chimera, divalent metal transporter, fission yeast, NRAMP.

INTRODUCTION

The mammalian *Nramp* (**N**atural **r**esistance **a**ssociated **m**acrophage protein) gene family is divided into two classes, *Nramp1* and *Nramp2*. *Nramp1* has been identified in the mouse *Bcg/Ity/Lsh* locus, which controls resistance to infection *in vivo* with *Mycobacterium*, *Salmonella* and *Leishmania* [1]. The *Nramp1* mRNA is expressed almost exclusively in phagocytic cells [1]. Nramp1 is a hydrophobic integral membrane protein, with the following predicted features: 12 putative transmembrane domains (TMD), two potential glycosylation sites and several phosphorylation sites [1–3], an N-terminal putative Src homology 3 (SH3)-binding domain [4] and a consensus 'the binding protein-dependent transport system inner membrane component signature' common to prokaryotic and eukaryotic transporters [5]. The cDNA and genomic DNAs for the corresponding human counterpart of *Nramp1* have been characterized [6–9]. It was demonstrated that the Nramp1 molecule is located on the late-endosomal and lysosomal compartment and the phagosome [10–12], and the N-terminal putative SH3-binding domain is associated with α- and β-tubulin of microtubules [13,14]. *Nramp2* was first identified as a homologue of *Nramp1* in mouse and human genomes [15–17]. The Nramp1 and Nramp2 proteins are highly similar (64% overall identity), with identical hydropathy profiles and predicted secondary structures. Unlike *Nramp1* mRNA, that of *Nramp2* is ubiquitously expressed [15]. Recently, Gunshin et al. [18] electrophysiologically identified a rat divalent metal transporter, *DMT1*, and found it to be an isoform of *Nramp2*. *Nramp2/DMT1* exhibits an unusually broad substrate range including Fe^{2+}, Zn^{2+}, Mn^{2+}, Cu^{2+}, Cd^{2+}, Co^{2+}, Ni^{2+} and Pb^{2+} and mediates active proton-coupled transport [18]. More recently, it has been shown that the microcytic anaemia (*mk*) mouse and the Belgrade (*b*) rat, which have inherited defects in iron transport that result in iron deficiency anaemia, have the same miss-sense mutations (G185R) in *Nramp2* [19,20]. These findings strongly suggested that *Nramp2/DMT1* is the apical iron transporter on intestinal epithelial cells and the endosomal transporter in transferrin-cycle endosomes. The *Nramp* family has been highly conserved during evolution and members have been found among other mammals, birds, insects, and even in plants, yeast and bacteria [2,3]. The budding yeast *Saccharomyces cerevisiae* has three Nramp-related proteins (*Smf1*, *Smf2*, *Smf3*) [21] that share approx. 40% identity to the mammalian Nramp proteins. *Smf1* was identified by Superk et al. [22] as a manganese transporter, and recent studies demonstrated that *Smf1* and *Smf2* additionally participate in the transport of other heavy metals including Cu^{2+}, Co^{2+} and Cd^{2+}, similarly to mammalian Nramp2 [23]. Pinner et al. [24] reported that, despite their large evolutionary distance, mouse Nramp2 can complement a double *smf1/smf2* yeast mutant and restore growth in the presence of EGTA and in the alkaline pH, but mouse Nramp1 cannot. These findings suggested that both mammalian Nramp2 and yeast *Smf* proteins are

Abbreviations used: A_{600}, absorbance at 600 nm; MM, minimal medium; PCR, polymerase chain reaction; CCD, charge coupled device; EGTA, ethyleneglycol-bis-(β-aminoethyl ether)-*N,N′*-tetraacetic acid; ORF, open reading frame; Nramp, natural resistance associated macrophage protein; TMD, transmembrane domain; DMT, divalent metal transporter; GFP, green fluorescent protein; ER, endoplasmic reticulum; MDR, multi-drug resistance.

[1] To whom correspondence should be addressed (e-mail fkishi-ygc@umin.ac.jp).

divalent metal transporters and this protein family has been structurally and functionally conserved during evolution. On the other hand, no divalent metal transport activity has been detected in Nramp1 despite the high degrees of similarity in primary sequence and secondary structure between Nramp1 and Nramp2. The function of Nramp1 at the molecular level is still unknown.

In this study, we have focused on whether NRAMP1 possesses divalent metal transport activity similarly to NRAMP2. We have taken advantage of the strong sequence homology and differential capacity of NRAMP1 and NRAMP2, and constructed four chimeric NRAMP genes by swapping the domains of human NRAMP1 and NRAMP2. The functional characteristics of wild-type NRAMP1, NRAMP2 and their chimeric constructs were investigated by expression in the divalent metal transporter-disrupted strain of fission yeast, *pdt1Δ*, and we analysed the divalent metal transport activity by complementation of the EGTA- and pH-sensitive phenotype of *pdt1Δ*.

EXPERIMENTAL

Strains and culture conditions

Standard recombinant techniques were performed using *Escherichia coli* strain JM109 and SCS110 (Stratagene) for *Bcl*I restriction-site-containing plasmids. *Schizosaccharomyces pombe* strain NOD1 (*h*$^+$ *leu1 his2 ura4 ade6-M216 inv1*) [25] was used for construction of the *pdt1Δ* strain. Standard rich medium, YPD (1 % yeast extract, 2 % peptone, 2 % glucose) and synthetic minimal medium (MM) for *S. pombe* cells were used as described elsewhere [26]. For repression of the *inv1* promoter, cells were grown in MM containing 8 % glucose (glucose medium). For derepression of the *inv1* promoter, cells were grown in MM containing 0.3 % glucose and 3 % glycerol (MM–glycerol medium). *S. pombe* cells were transformed by the lithium acetate method as described previously [27].

Isolation and disruption of the *pdt1*$^+$ gene

The *pdt1*$^+$ gene was cloned by PCR from fission yeast genomic DNA using primers based on the sequence deposited in the *S. pombe* genome database: *pdt1*$^+$ sense 5′-TGATCACCCATGTCTAGCCAATCCTA-3′ and antisense 5′-TGATCAATTTAGAAGGAGACTCCCAT-3′ where *Bcl*I sites are underlined. Reaction product was purified by agarose gel electrophoresis and cloned into the T-vector. Nucleotide sequences of the PCR products in this study were verified by the dideoxynucleotide chain-termination method using an LI-COR 4000L automated DNA sequence. A null allele of *pdt1*$^+$ was constructed as follows: the 1.5-kb fragment containing *pdt1*$^+$ was digested with *Bam*HI, and the *Bam*HI-digested *ura4*$^+$ gene was inserted into the cleaved *pdt1*$^+$ gene. A linearized DNA fragment carrying this disrupted *pdt1*$^+$ gene was used to transform a wild-type haploid strain, and *ura*$^+$ transformants were selected and confirmed by Southern hybridization.

Vectors and plasmid constructions

To express the human NRAMP family gene in *S. pombe*, the expression vector pFML2-GFP using the promoter of the fission yeast glucose repression gene, *inv1*$^+$ [28] was constructed as follows: oligonucleotide-directed mutagenesis [29] of pAL-*inv1*$^+$p containing the 3.6-kb *Pst*I–*Bam*HI fragment of *inv1*$^+$ was used to insert a *Bam*HI site immediately before the initiation codon of *inv1*$^+$. The oligonucleotide, 5′-TTTGAAGATTGGATCCAATG-TTTTT-3′ with a *Bam*HI site was used as a primer for oligonucleotide-directed mutagenesis of pAL-*inv1*$^+$p to generate pFML2. The *Bam*HI–*Not*I fragment containing the green fluorescent protein (GFP) gene from pEGFPN1 (Clontech) was cloned into *Bam*HI–*Not*I sites present in the pFML2 plasmid to generate pFML2-GFP. The human *NRAMP1* cDNA was amplified using the sense primer, NR1-1: 5′-GGATCCTCAATGACAGGTGACAAGGGT-3′ [possesses a 5′ *Bam*HI site (underlined) and the first six amino acids including the initiation methionine (double-underlined) of NRAMP1] and the antisense primer, NR1-2: 5′-GGATCCAAGCCAGAGGTCTCCCC-3′ [possesses a 5′ *Bam*HI site (underlined) and the final five amino acids of NRAMP1]. The reaction product was digested with *Bam*HI and the digestion product was cloned into pUC12. The resulting plasmid pNRAMP1 was digested with *Bam*HI, and the *Bam*HI fragment containing the full-length *NRAMP1* cDNA was ligated into the *Bam*HI site of pFML2-GFP to generate pFML2-NRAMP1-GFP. The human *NRAMP2* cDNA was amplified using the sense primer, NR2-1: 5′-TGATCAACCATGGTGCTGGGTCCTGA-3′ [possesses a 5′ *Bcl*I site (underlined) and the first six amino acids including the initiation methionine (double-underlined) of *NRAMP2*] and the antisense primer, NR2-2: 5′-TGATCATG-TAATTTAACGTAGCCACG-3′ [possesses a 5′ *Bcl*I site (underlined) and the final five amino acids of *NRAMP2*]. The reaction product was purified by agarose gel electrophoresis and cloned into the T-vector. The resulting plasmid, pNRAMP2 was digested with *Bcl*I, and the *Bcl*I fragment containing the full-length *NRAMP2* cDNA was ligated into the *Bam*HI site of pFML2-GFP to generate pFML2-NRAMP2-GFP.

Construction of *NRAMP1* and *NRAMP2* chimeric genes

Chimeras were constructed by using both engineered sites introduced through site-directed mutagenesis (GeneEditer™ *in vitro* Site-Directed Mutagenesis System, Promega) and native restriction sites. Oligonucleotide swap1: 5′-TCAGCCTGCGCAGCTATGGG-3′ was used to introduce *Fsp*I from *NRAMP1* cDNA into the pNRAMP1, and the mutated plasmid was designated as pSwap1. Oligonucleotide swap2: 5′-CCCAGAGTTTGCGCAAGCTAAAAC-3′ was used to introduce an *Fsp*I site from *NRAMP2* cDNA into pNRAMP2 and the mutated plasmid was designated as pSwap2. The *Bam*HI–*Fsp*I 174-bp fragment from pSwap1 encoding the N-terminal cytoplasmic domain of NRAMP1 and the *Fsp*I–*Bcl*I 1615-bp fragment from pSwap2 encoding amino acids 68–561 of NRAMP2 were ligated. PCR was performed using the ligation product as the template and oligonucleotide NR1-3: 5′-TGATCA-TCAATGACAGGTGACAAGGGT-3′ [possesses a 5′ *Bcl*I site (underlined) and the first six amino acids including the initiation methionine (double-underlined) of NRAMP1] and NR2-2 as primers, and then the PCR product was cloned into the T-vector to generate pNRAMP122. The *Bcl*I–*Fsp*I 210-bp fragment of pSwap2 encoding the N-terminal cytoplasmic domain of NRAMP2 and the *Fsp*I–*Bam*HI 1614-bp fragment from pSwap1 encoding amino acids 57–550 of NRAMP1 were ligated. PCR was performed using the ligation product as the template and oligonucleotides NR2-1 and NR1-2 as primers and the PCR product was cloned into the T-vector to generate pNRAMP211. A unique *Sac*I restriction site, which appears at identical positions in the wild-type *NRAMP1* and *NRAMP2* cDNA, was used to generate *NRAMP221* and *NRAMP212* with the fusion point at the middle of the fourth internal loop. The chimeric cDNA, *NRAMP221*, was constructed by exchanging the C-terminal *Sac*I–*Sac*I 0.5-kb fragment of *NRAMP2* with that of *NRAMP1*. The chimeric cDNA *NRAMP212* was constructed by exchanging the C-terminal *Sac*I–*Sac*I 0.5-kb fragment of *NRAMP211* for

that of *NRAMP2*. The chimeric constructs were digested with *Bam*HI–*Bcl*I or *Bcl*I and the fragment containing the cDNA was ligated into the *Bam*HI site of pFML2-GFP.

Preparation of anti-NRAMP1 N-specific and NRAMP2 N-specific antisera

A fusion between the *E. coli trpE* gene and the *NRAMP1* gene was constructed by subcloning a 174-bp *Bam*HI–*Fsp*I fragment from pSwap1 encoding amino acids 1–56 of the human *NRAMP1* into *Bam*HI–*Sma*I-digested pATH3, generating an in-frame fusion gene. A fusion between the *trpE* and the *NRAMP2* gene was constructed by subcloning the 210-bp *Bcl*I–*Fsp*I fragment from pSwap2 encoding amino acids 1–66 of human *NRAMP2* into *Bam*HI–*Sma*I-digested pATH3, generating an in-frame fusion gene. Induction of the trpE-NRAMP1$^{1\text{-}56}$ and trpE-NRAMP2$^{1\text{-}66}$ fusion proteins was accomplished as previously described by Kleid et al. [30]. Sodium dodecyl sulphate/polyacrylamide gel electrophoresis (SDS/PAGE) revealed prominent 43- and 51-kDa bands representing the trpE-NRAMP1$^{1\text{-}56}$ and trpE-NRAMP2$^{1\text{-}66}$, respectively, which were excised and electroeluted from the gel slices with an Atto AE-3590 electrochamber. Aliquots of approx. 1 mg of the fusion proteins were emulsified with Freund's complete adjuvant and injected intramuscularly or subcutaneously into young male New Zealand White rabbits. Antisera (designated as anti-NRAMP1 N Ab, and anti-NRAMP2 N Ab antiserum, respectively) were collected and stored at −80 °C.

Immunoblotting

Transformed yeast cells were grown to mid-log phase in glucose medium. Cells were washed with PBS and resuspended in glycerol medium for induction of recombinant proteins followed by incubation for 12 h. Induced cells (30 A_{600}) were collected by centrifugation and resuspended in 0.2 ml of 1 M sorbitol–10 mM EDTA, 10 mM DTT, and the cells were incubated at 30 °C for 10 min. Aliquots of 2 μl of Zymolyase 100T (20 mg/ml) and Novozyme 234 (20 mg/ml) were added, and the cells were incubated at 30 °C for 30 min. Incubated cells were washed twice with ice-cold 1 M Sorbitol/10 mM EDTA and resuspended in 0.2 ml of lysis buffer (50 mM Tris, pH 8.0, 150 mM NaCl, 5 mM EDTA, 1 mM PMSF). Cells were disrupted using acid-washed glass beads and spun for 5 min at 5000 ***g***. The supernatant was spun for an additional 30 min at 128000 ***g*** to recover the pellet as the membrane fraction. The membrane fraction was resolved in 100 μl of Laemmli's sample buffer and aliquots of 5 μl were resolved by 10 % SDS/PAGE. Proteins were transferred onto nitrocellulose membranes, and the blots were incubated with the primary antibodies. The proteins were detected with horseradish peroxidase-conjugated antibody against rabbit IgG (Amersham Pharmacia).

Fluorescence microscopy

Transformed yeast cells were grown to mid-log phase in glucose medium. Cells were washed with PBS, resuspended in glycerol medium and then incubated for 12 h. Cells were harvested, concentrated by centrifugation and resuspended in PBS. Resuspended cells were stained with Hoechst 33342 [31], and with FM4-64 [32]. The fluorescence in non-fixed cells was observed using an Olympus BX50 microscope. Photographs were taken with an Olympus colour chilled 3CCD camera M-3204C-10. Images were acquired with the Adobe Photoshop™ 4.0J (Adobe Systems Inc.).

RESULTS

Isolation and characterization of fission yeast divalent metal transporter gene

By examination of the *S. pombe* Genome Database, the gene product was predicted to encode a protein homologous to the NRAMP family. A gene in chromosome 1 (SPAC27F1.08) revealed a single contiguous ORF potentially encoding a 521 amino acid protein, the gene product of which shows overall identity of 30.1 % to human NRAMP1 and 31.9 % to human NRAMP2, and of 46.7 and 45.2 % to *Saccharomyces cerevisiae* divalent metal transporters *Smf1* and *Smf2*, respectively. We found no other homologues in the *S. pombe* Genome Database at that time. Based on the similarity to other divalent metal transporters, we supposed that this gene product might be a divalent metal transporter in *S. pombe*, and designated this gene as *pdt1*$^+$ (for *S. **p**ombe* **d**ivalent metal **t**ransporter gene).

To examine the phenotypic consequences of a null allele of *pdt1*$^+$, we performed gene deletion-disruption of this locus. A linear fragment of the *pdt1*$^+$ gene into which was inserted the *S. pombe ura4*$^+$ gene (Figure 1A) was used to transform haploid strain NOD1 (see Experimental section). Several *ura*$^+$ transformants were isolated and the structure of the disrupted allele was verified by Southern blotting analysis (Figure 1B). The *pdt1Δ* cells grew well at 30 and 36 °C, and did not exhibit a temperature-sensitive growth defect (data not shown). The *S. cerevisiae smf1* gene homologous to *pdt1*$^+$ has been proposed to function as a Mn^{2+} transporter, and a yeast strain carrying a null allele at *smf1* cannot grow on medium containing the divalent cation chelator, EGTA at 12.5 mM [22]. We examined whether deleting the *pdt1*$^+$ gene conferred sensitivity to EGTA. Both wild-type and *pdt1Δ* strains were spotted onto plates containing various concentrations of EGTA and the growth of these strains was examined. Growth inhibition of *pdt1Δ* was observed and this inhibition was dependent on EGTA concentration in the medium (Figure 1C). The *pdt1*Δ strain could not grow on medium containing 7.5 mM EGTA. We also examined the growth defect of *pdt1Δ* in liquid medium containing 7.5 mM EGTA. After 37 h of incubation, significant growth inhibition was observed in *pdt1Δ* cells (Figure 1D). This growth defect of the *pdt1Δ* strain was complemented by transformation with the expression plasmid pFML2 carrying the full-length *pdt1*$^+$ ORF (Figure 1D). These results suggested that the EGTA-sensitive phenotype of *pdt1*Δ is caused by deletion of the *pdt1*$^+$ gene, and that the *pdt1*$^+$ gene is a functional divalent metal transporter in *S. pombe*. This EGTA-sensitive phenotype of the *pdt1Δ* strain allowed us to perform functional analysis of human NRAMP family genes in fission yeast.

Expression of human NRAMP1, NRAMP2 and their chimeras in fission yeast

(i) Construction of the heterogeneous gene expression system in fission yeast

To express human NRAMP family proteins in fission yeast, we initially attempted to use the expression plasmid pART1 using a strong *S. pombe adh1* promoter [33]. Human *NRAMP1* cDNA was cloned into the *Bam*HI restriction site of pART1 to generate pART1-*NRAMP1*, and transformed into *S. pombe pdt1Δ*. However, no transformants were obtained. It was thus considered that the overexpression of polytypic membrane proteins such as NRAMP1 under the control of the strong *adh1* promoter could be toxic to the cells. Then, we constructed an expression vector pFML2-GFP carrying the promoter of the fission yeast glucose-repressible gene *inv1*$^+$ [28] to regulate the expression level (see

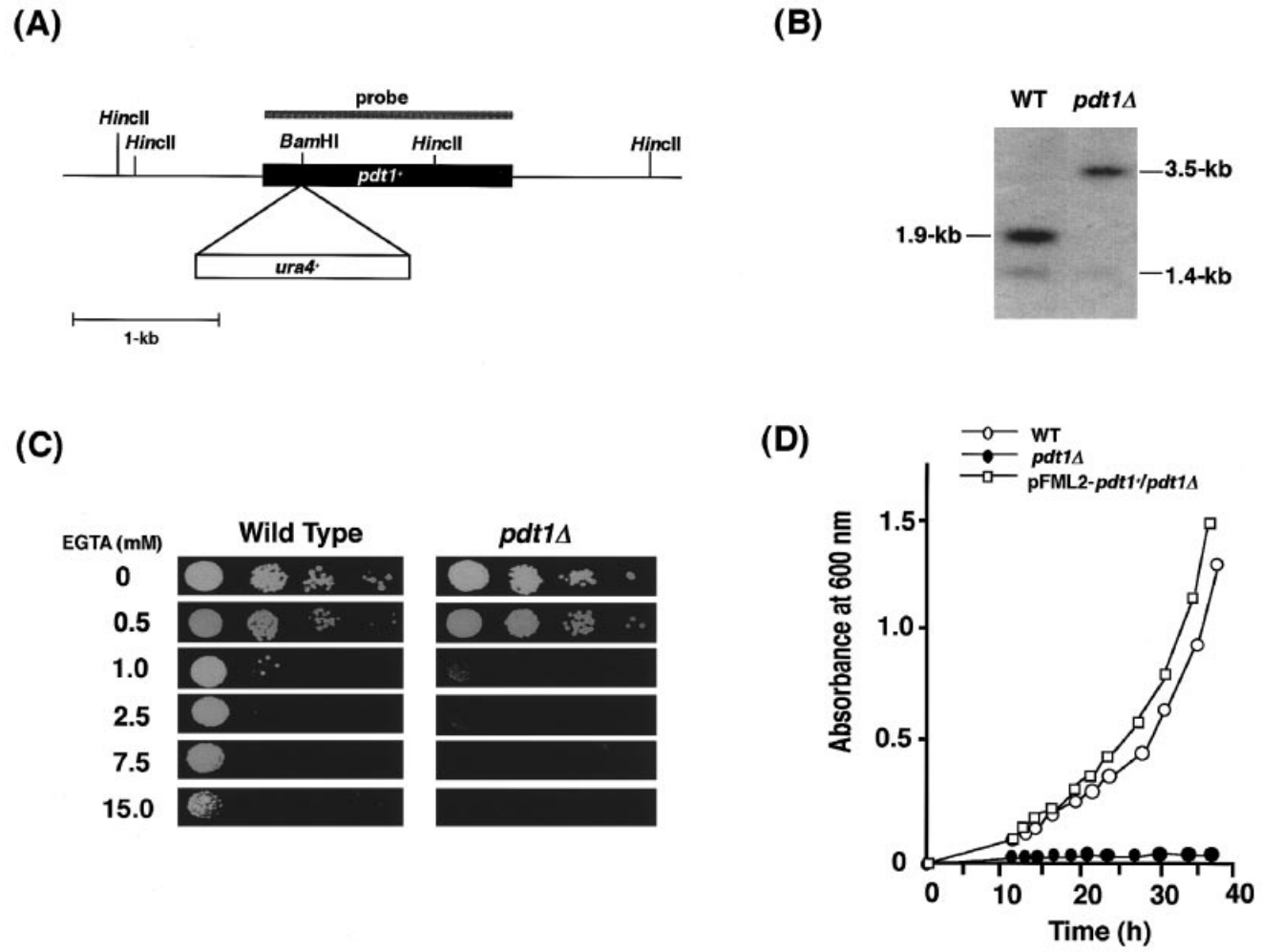

Figure 1 Characterization of fission yeast divalent metal transporter *pdt1*$^+$

(**A**) Restriction map and gene disruption of the *pdt1*$^+$ locus. (**B**) Southern blotting analysis of the *pdt1*$^+$ gene disruption mutant. Genomic DNA was isolated from *S. pombe* wild-type strain NOD1 and disruption mutant strain *pdt1Δ* digested with *Hin*cII. The digested DNA (5 μg) was separated on a 1.0% agarose gel. Following denaturation, the DNA was transferred onto Hybond N$^+$ and the blots were hybridized with the 1.6-kb *Bc*/I fragment of full-length *pdt1*$^+$ ORF as a probe. (**C**) EGTA sensitivity assay of wild-type and *pdt1Δ* strain on plates. Wild-type and *pdt1Δ* strain grown in glucose medium to mid-log phase were diluted in sterile distilled water and spotted onto glycerol plates containing various concentrations of EGTA. The spots contained 10^4, 10^3, 10^2 or 10^1 cells. (**D**) EGTA sensitivity assay of wild-type, *pdt1Δ* strain and Pdt1-expressing *pdt1Δ* on liquid media. Cells grown in glucose medium to mid-log phase were diluted in 100 ml of glycerol medium containing 7.5 mM EGTA to $A_{600} = 0.05$. The samples were grown at 30 °C, and time-dependent growth was determined by measuring A_{600}.

Experimental section). *S. pombe pdt1*$^+$, human *NRAMP1* and *NRAMP2* ORF were cloned into the *Bam*HI restriction site of pFML2-GFP and the GFP was tagged in-frame to the C termini of these proteins. These plasmids were then used to transform *pdt1Δ* strain. The recombinant proteins expressed in *S. pombe* were detected by monitoring the fluorescence of GFP. In all of the transformants, we observed GFP fluorescence under the condition of glucose derepression (data not shown). Therefore, the NRAMP proteins could be expressed in fission yeast under the present experimental conditions.

(ii) Construction of four chimeras composed of regions of NRAMP1 and NRAMP2

Pinner et al. [24] reported that mouse *Nramp2* could complement the hypersensitive phenotype to EGTA of *S. cerevisiae smf1/smf2* double-disrupted strain, but mouse *Nramp1* could not. Gunshin et al. reported that ^{55}Fe uptake in *Xenopus* oocyte-expressing NRAMP1 showed a different profile from that in those expressing NRAMP2/DMT1, and the affinity for Fe^{2+} of NRAMP1 seemed much lower than that of NRAMP2/DMT1 [18, personal communication]. There is no clear evidence that the NRAMP1 molecule possesses the divalent metal transport activity except for its sequence homology to NRAMP2/DMT1. The *NRAMP1* and *NRAMP2* genes encode highly homologous polypeptides which share the predicted structural features shown in Figure 2. We constructed two chimeras, NRAMP211, and NRAMP122, swapping the N-terminal cytoplasmic domains (Figure 2). Using the unique *Sac*I site located in the middle of the fourth cytoplasmic loop in each sequence, we also constructed two additional chimeras; NRAMP221 was composed of the N-terminal first 8 TMD of NRAMP2 and the C-terminal part of NRAMP1 and NRAMP212 was composed of the N-terminal cytoplasmic domain of NRAMP2 and the TMD 1-8 of NRAMP1 and the C-terminal part of NRAMP2 (Figure 2). These chimeras were cloned into pFML2-GFP. GFP was tagged in-frame to their C-

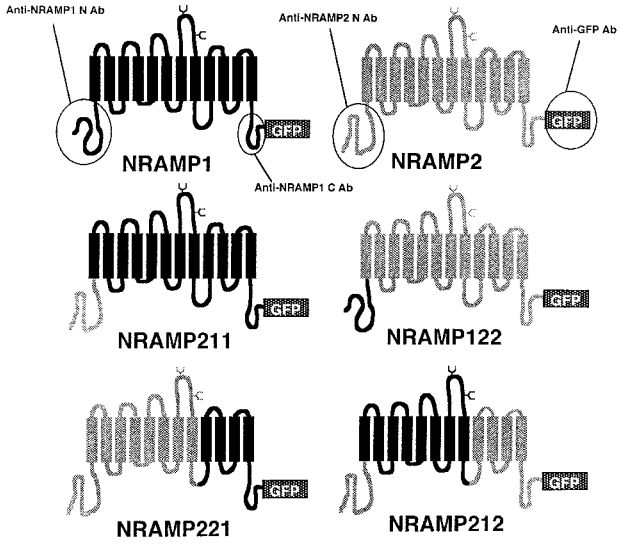

Figure 2 Construction of NRAMP1 and NRAMP2 chimeric genes

Predicted secondary structures of wild-type and chimeric mutants.

termini and transformed into *pdt1Δ* strain. These transformants were tested for complementation of the EGTA-sensitive phenotype of *pdt1Δ*.

Functional analysis of NRAMP1, NRAMP2 and their chimeras in fission yeast

(i) Complementation of EGTA-sensitive phenotype of *pdt1Δ* by human NRAMP2

We examined whether the human wild-type NRAMPs and the chimeric NRAMPs could complement the EGTA-sensitivity of fission yeast divalent metal transporter disrupted-strain, *pdt1Δ*. Transformants were grown in glucose medium, and then spotted onto glycerol plates containing various concentrations of EGTA. After incubation at 30 °C for 5 days, vector alone (GFP) transformants exhibited the EGTA-sensitive phenotype and these cells could not grow on plates containing 7.5 mM EGTA (Figure 3A). Significant complementation of EGTA sensitivity was observed in pdt1-GFP and NRAMP2-GFP transformants (Fig. 3A). NRAMP1-GFP, NRAMP211-GFP, NRAMP221-GFP and NRAMP212-GFP transformants were unable to restore the EGTA-sensitive phenotype of *pdt1Δ* (Figure 3A). The numbers of surviving cells in NRAMP122-GFP transformants on 1.0 mM and 2.5 mM EGTA plates were much greater than those of GFP, NRAMP1-GFP and other chimeric GFP transformants (Figure 3A). To verify that this survival on plates containing 2.5 mM EGTA truly reflected cellular resistance to EGTA of the NRAMP122-GFP transformants, further investigations to test the EGTA-sensitivity in liquid medium were performed. When cells were grown in glycerol medium without EGTA, there were no differences in cell growth rate. When cells were grown in 7.5 mM EGTA, significant growth inhibition was observed in all of the transformants except pdt1-GFP and NRAMP2-GFP (Figure 3B). When cells were grown in 2.5 mM EGTA, restoration of the cell growth was observed in NRAMP122-GFP transformant. We concluded that NRAMP122-GFP restores the EGTA sensitivity of *pdt1Δ* cells, although its complementation level was much lower than that of wild-type NRAMP2-GFP.

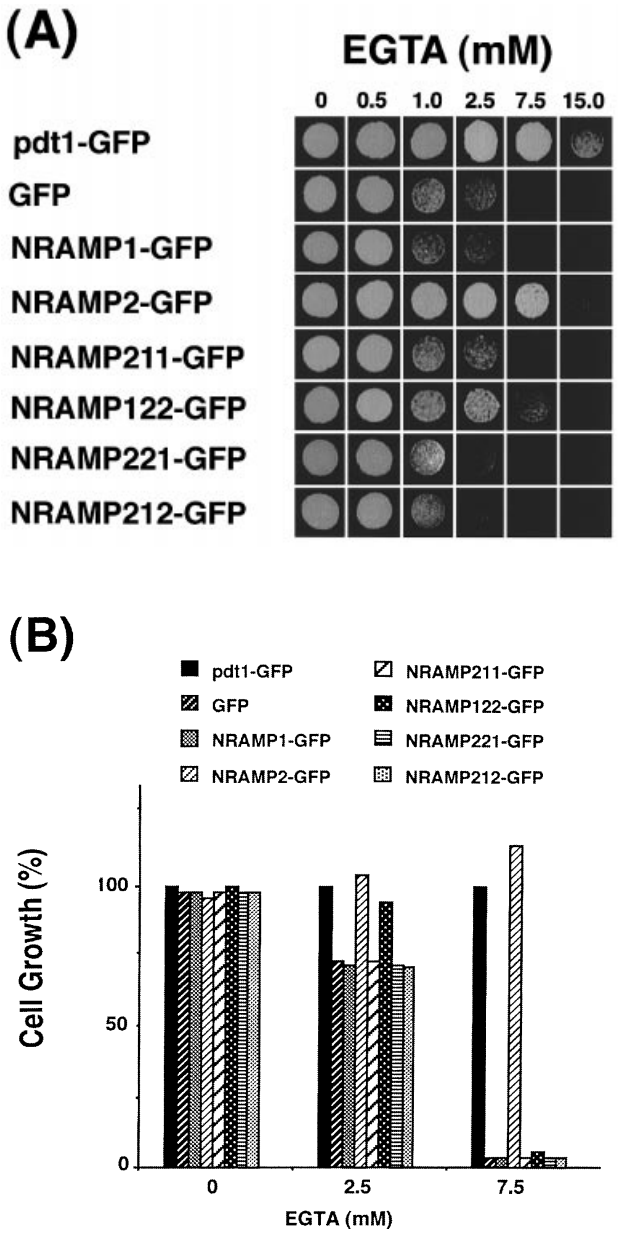

Figure 3 EGTA-sensitivity assay of the *pdt1Δ* strain with wild type *pdt1*$^+$, NRAMP1 and NRAMP2 and various chimeric constructs

(**A**) The fission yeast divalent metal transporter-disrupted strain *pdt1Δ*, transformed with pFML2-GFP expression plasmid alone (GFP), pFML2-GFP carrying either *pdt1*$^+$ (pdt1-GFP), wild-type human *NRAMP1* (NRAMP1-GFP) or *NRAMP2* (NRAMP2-GFP), or chimeras of *NRAMP211* (NRAMP211-GFP), *NRAMP122* (NRAMP122-GFP), *NRAMP211* (NRAMP221-GFP), or *NRAMP212* (NRAMP212-GFP) were grown in glucose medium to mid-log phase, and cells were counted and diluted with PBS. Samples containing 10^4 cells were spotted onto MM–glycerol plates containing various concentrations of EGTA and the plates were incubated at 30 °C for 5 days. (**B**) Cells grown in glucose medium to mid-log phase were diluted in 100 ml of glycerol medium containing 0, 2.5 or 7.5 mM EGTA to $A_{600} = 0.05$. The samples were incubated at 30 °C until pdt1-GFP transformants reached mid-log phase (1.0–1.2). The A_{600} of pdt1-GFP transformant in conditions was arbitrarily set at 100%.

(ii) Complementation of pH-sensitive phenotype of *pdt1Δ* by human NRAMP2

Pinner et al. [24] reported that *S. cerevisiae smf1/smf2* double-disrupted strain was hypersensitive to alkaline pH (pH 7.9) and

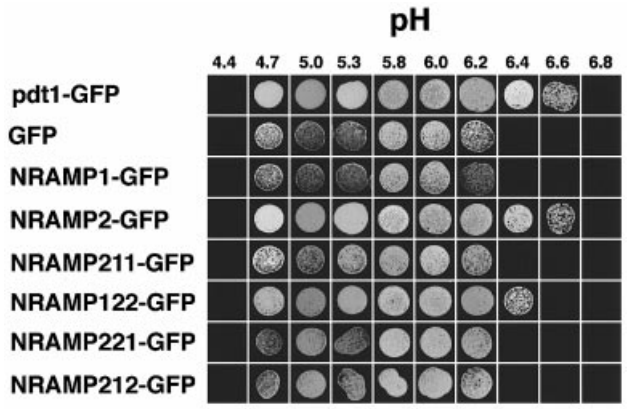

Figure 4 pH-sensitivity assay of the *pdt1Δ* strain with wild type *pdt1*$^+$, NRAMP1 and NRAMP2 and various chimeric constructs

The fission yeast divalent metal transporter-disrupted strain *pdt1Δ*, transformed with pFML2-GFP expression plasmid alone (GFP), pFML2-GFP carrying either *pdt1*$^+$ (pdt1-GFP), wild-type human *NRAMP1* (NRAMP1-GFP) or *NRAMP2* (NRAMP2-GFP), or chimeras of *NRAMP211* (NRAMP211-GFP), *NRAMP122* (NRAMP122-GFP), *NRAMP221* (NRAMP221-GFP), or *NRAMP212* (NRAMP212-GFP) were grown in glucose medium to mid-log phase, and cells were counted and diluted with PBS. Samples containing 10^4 cells were spotted onto YP (1% yeast extract, 2% peptone)–glycerol medium buffered with 50 mM Na acetate buffer (pH 4.4–5.3) or 50 mM Na phosphate buffer (pH 5.8–6.8) and incubated at 30 °C for 4 days.

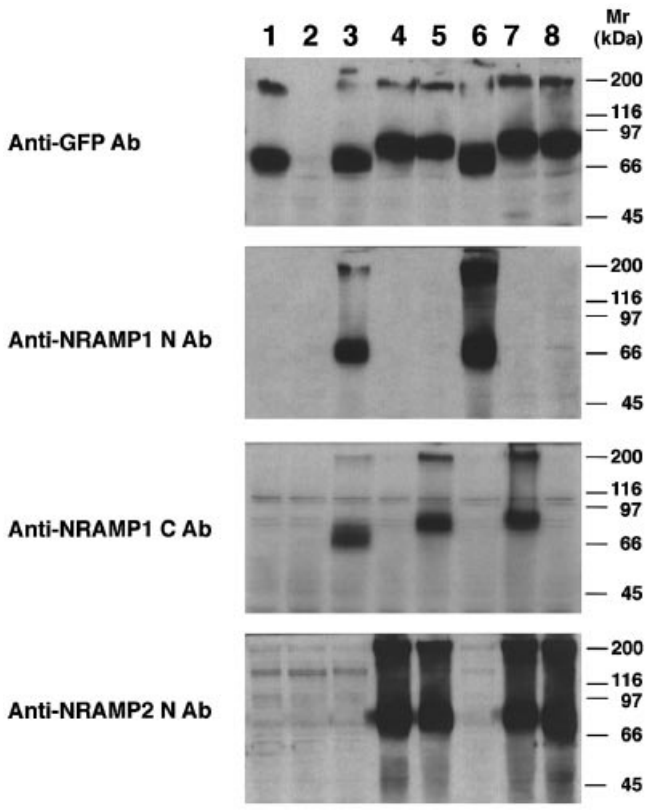

Figure 5 Detection of GFP-tagged wild-type Pdt1, NRAMP1, NRAMP2 and the various chimeric proteins expressed in fission yeast

S. pombe strain *pdt1Δ* was transformed with pFML2-GFP expression plasmid alone (lane 2) or pFML2-GFP containing full-length ORF of *pdt1*$^+$ (lane 1), wild-type human *NRAMP1* (lane 3) or *NRAMP2* (lane 4), or chimeric constructs *NRAMP211* (lane 5) or *NRAMP122* (lane 6), or *NRAMP221* (lane 7), or *NRAMP212* (lane 8). All proteins were tagged by the in-frame addition of green fluorescent protein (GFP) at their C terminus. Membrane fractions were prepared from each transformant, separated by 10% SDS/PAGE, and analysed by immunoblotting with the anti-GFP polyclonal antibody used at a 1/500 dilution, anti-NRAMP1 N Ab, 1/2000, or anti-NRAMP1 C Ab, no. 12766 (35), 1/2000, or anti-NRAMP2 N Ab, 1/2000 and a secondary horseradish peroxidase-conjugated antibody against rabbit IgG, 1/2000 (Amersham Pharmacia).

mouse *Nramp2* could complement pH-sensitive phenotypes. We examined whether the *S. pombe pdt1Δ* strain showed the hypersensitivity to growth at high pH, and human NRAMP2 and its chimeras could complement the pH-sensitive phenotype. Both wild-type and *pdt1Δ* strains were spotted onto plates with various pH ranges (4.4–6.8) and the growth of these strains was examined. Even wild-type cells could not grow when the medium pH was below 4.4 and above 6.8 (Figure 4). Growth inhibition of *pdt1Δ* was observed when the medium pH was above 6.4 as compared with wild type, and essentially the same results were obtained in the presence of vector alone (GFP), NRAMP1-GFP, NRAMP211-GFP, NRAMP221-GFP, or NRAMP212-GFP (Figure 4). This pH-sensitive phenotype of *pdt1Δ* strain was complemented by the expression of pdt1-GFP and NRAMP2-GFP (both pH 6.4 and 6.6) and partly NRAMP122-GFP (only pH 6.4) (Figure 4). The complementation by human NRAMPs and their chimeras on the pH-sensitive plate assay was similar to that of the EGTA-sensitive plate assay (Figure 3A). Notably, the complementation activity of NRAMP122 was well demonstrated as compared with the result obtained by the EGTA-sensitive plate assay (Figure 4).

Identification of NRAMP proteins expressed in fission yeast

To eliminate the possibility that the lack of complementation activity of NRAMP1 and the chimeras was due to the lack of expression or degradation of recombinant proteins in these cells, immunoblotting analysis was performed using antibodies to GFP (anti-GFP Ab), to NRAMP1 C-terminal specific peptide [35] (no. 12766, anti-NRAMP1 C Ab), to trpE-NRAMP1$^{1-56}$ (anti-NRAMP1 N Ab) and to trpE-NRAMP2$^{1-66}$ (anti-NRAMP2 N Ab) raised in this study. Anti-GFP Ab recognized specific bands in the membrane fractions of all except GFP transformants (Figure 5), in which GFP was present in the cytosolic fraction (data not shown). A specific immunoreactive band of 68–72 kDa was detected in pdt1-GFP, NRAMP1-GFP and NRAMP122-GFP transformants (lanes 3 and 6 of Figure 5, respectively) and a specific immunoreactive band of 76–80 kDa was detected in NRAMP2-GFP, NRAMP211-GFP, NRAMP221-GFP and NRAMP212-GFP transformants (lanes 4, 5, 7, 8 of Figure 5, respectively). An additional immunoreactive band with a molecular mass of approx. 200 kDa was detected in all transformants. As this 200-kDa band was also observed in cells cultured in the presence of the N-glycosylation inhibitor tunicamycin (data not shown), this band may not have been a hyperglycosylated form of the molecules but may have corresponded to multimers of NRAMP proteins caused by aggregation. Anti-NRAMP1 N Ab recognized specific bands of the same molecular mass as detected by anti-GFP Ab in NRAMP1-GFP and NRAMP122-GFP transformants (Figure 5). Anti-NRAMP1 C Ab recognized specific bands of the same molecular mass as detected by anti-GFP Ab in NRAMP1-GFP, NRAMP211-GFP, and NRAMP221-GFP transformants (Figure 5). Anti-NRAMP2 N Ab recognized specific bands of the same molecular mass as detected by anti-GFP Ab in NRAMP2-GFP, NRAMP211-GFP, NRAMP221-GFP and NRAMP212-GFP transformants (Figure 5). These results were consistent with the predicted signal pattern from these constructs. The

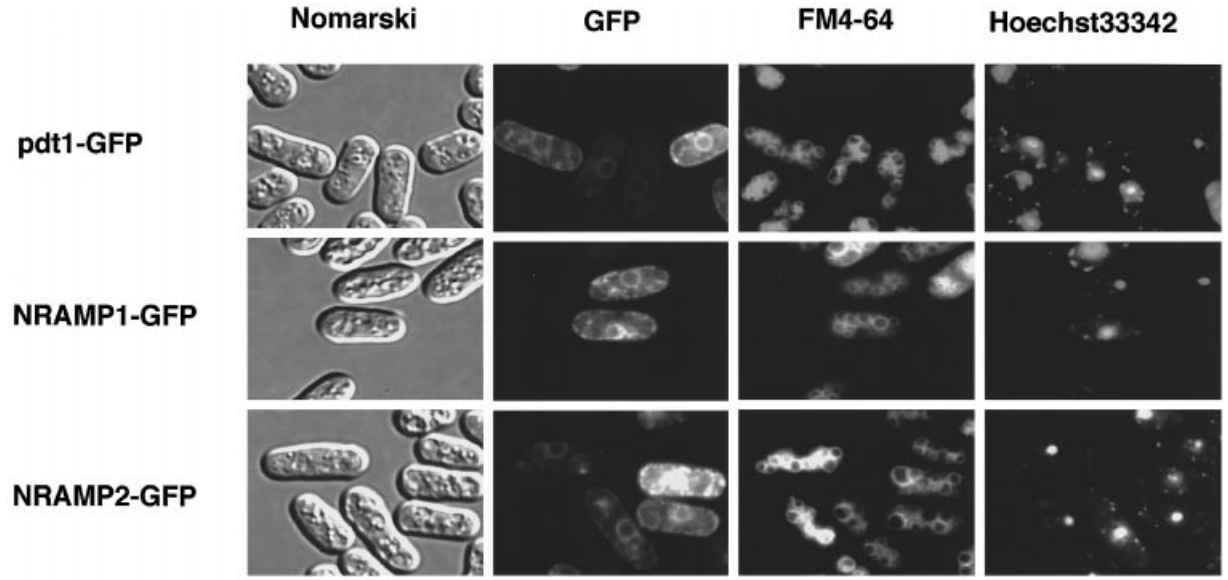

Figure 6 Localization of NRAMP proteins in fission yeast

The transformed cells were stained with Hoechst 33342 for visualization of nucleic acids, and FM4-64 for visualization of the vacuolar membrane. The stained cells were examined by fluorescence microscopy. Expressions of pdt1-GFP, NRAMP1-GFP and NRAMP2-GFP was under the control of the *inv1* promoter and induced by growth in glycerol media.

expression level was equivalent among these transformants, and we concluded that neither lack of protein expression nor degradation of the recombinant proteins occurred.

Localization of NRAMP proteins in fission yeast

To investigate the protein sorting in cells expressing the recombinant GFPs, the subcellular localization of these proteins was examined by fluorescence microscopic analysis of naturally fluorescent GFP. As shown in Figure 6, pdt1-GFP expressed in fission yeast exhibited a light double ring-like signal surrounding both the nucleus (defined by Hoechst 33342) and the cell surface. This pattern demonstrated the localization of this molecule in the endoplasmic reticulum (ER) and at the cell surface. Most of the cells exhibited the double ring-like signal, and a few cells exhibited signals in the vacuolar membrane (defined by FM4-64) (approx. $< 10\,\%$ of transformants) (data not shown). The same fluorescent pattern was observed in NRAMP1-GFP and NRAMP2-GFP (Figure 6) and other chimeras (data not shown) expressed in fission yeast. These observations indicated that all of the recombinant NRAMP proteins examined had the same subcellular localization in fission yeast, and the lack of the complementation of NRAMP1 and other chimeras in fission yeast was not due to their subcellular localization but to structural differences.

DISCUSSION

Previously, we reported cloning of cDNA and genomic clones of human *NRAMP1* and *NRAMP2* [6,7,17,34]. Comparison of the genomic structure and the primary sequence of human NRAMP1 and NRAMP2 led us to hypothesize that the modern NRAMP genes may have arisen from a common ancestor and have acquired specific N-terminal cytoplasmic domains during evolution, conferring specific function(s) on each protein. Based on this hypothesis, we supposed that swapping of the N-terminal cytoplasmic domains of NRAMP1 and NRAMP2 may be able to exchange their functions. Therefore we constructed four chimeric NRAMP genes by swapping the domains with each other. The functional characteristics of wild-type NRAMP1, NRAMP2 and their chimeric constructs were examined by expression in the fission yeast divalent metal transporter-disrupted strain *pdt1Δ*, and analysing the divalent metal transport activity by complementation of the EGTA- and pH-sensitive phenotype of *pdt1Δ*. The fission yeast Pdt1, human NRAMP1, NRAMP2 proteins and their chimeras expressed in fission yeast were recovered in the membrane fractions, and fluorescent microscopy demonstrated that these proteins were localized to both the ER and the cell surface. The NRAMP1-GFP and NRAMP2-GFP proteins were detected by immunoblotting with anti-GFP Ab or specific antibodies as bands with apparent molecular masses of 68–72 and 76–80 kDa, respectively (Figure 5, lanes 3 and 4). The difference in the molecular mass between NRAMP1 and NRAMP2 was 2 kDa calculated from the deduced amino acid sequences. However, the actual difference in the molecular mass was 8–10 kDa as determined by their electrophoretic mobility on SDS/PAGE. Replacement of the N-terminal cytoplasmic domains resulted in significant alterations in electrophoretic mobility (Figure 5). This occurred only in exchanging the N-terminal cytoplasmic domains with each other. The same observation was seen with the electrophoretic mobilities of fusion proteins of trpE or GST and the N-terminal cytoplasmic domains of NRAMPs (data not shown). It indicated that their N-terminal cytoplasmic domains may have the characteristic structures including the differences in the electrophoretic.

We found that human NRAMP2 is able to completely complement the EGTA- and pH-sensitive phenotype of *pdt1Δ*, but that human NRAMP1 is not. These results are consistent with the results of complementation analysis of mouse Nramp1 and Nramp2 in *S. cerevisiae smf1/smf2* double mutant [24]. Of our chimeric constructs, only NRAMP122-GFP containing the N-terminal cytoplasmic domain of NRAMP1 in place of that of NRAMP2 could weakly restore the EGTA- and pH-sensitivity of *pdt1Δ*, although the complementation level was much lower than that of wild-type NRAMP2. This result suggested that the functional differences between NRAMP1 and NRAMP2 are

located in these regions. However, results obtained with the reverse construct, NRAMP211, indicated that these regions are not solely responsible for the differences in EGTA- and pH-sensitivity of NRAMP1 and NRAMP2, and suggested that additional protein domain(s) located elsewhere in NRAMP1 may be responsible for the functional differences from NRAMP2. Furthermore, additional chimeric constructs, NRAMP221 and NRAMP212, recombinant NRAMP2 in which the C-terminal (TMD9–12 and C-terminal cytoplasmic domain), or N-terminal domain (TMD1–8) was replaced with the homologous region of NRAMP1, respectively, could not complement the EGTA- and pH-sensitivity of *pdt1Δ*. In the present study of NRAMP1 and NRAMP2, we found no evidence that the NRAMP1 molecule possessed divalent metal transport activity. These results led us to two hypotheses. The NRAMP1 molecule may possess potential divalent metal transport activity, but its activity may be tightly regulated by other regulatory factors, binding of unidentified protein(s) or phosphorylation, etc. In our previous studies, we showed that the N-terminal cytoplasmic domain of the NRAMP1 molecule is associated with α- and β-tubulin of microtubules and the NRAMP1 molecule is a new type of microtubule-associated protein [13,14]. Barton et al. [4] reported that the N-terminal cytoplsmic domain of the NRAMP1 molecule is a putative SH3-binding domain, which shares 55 % identity to that of *Drosophila* dynamin. The SH3-binding domain of the large GTPase dynamin is associated with microtubules [36,37] and various proteins containing SH3 domains such as Grb2/Ash [38], amphiphysin [39] and PLC-γ [40], and the binding activity of microtubules and SH3 domains is stimulated by the GTPase activity of dynamin *in vitro* [41–43]. Although the function of dynamin is quite different from the predicted function of the [1] molecule, the microtubule-binding abilities of these two molecules suggests that similar regulatory mechanisms of their activity may be involved in their functional expression. Therefore, we speculated that NRAMP1 divalent metal transport activity may be regulated by microtubules or other as yet unidentified proteins containing SH3 domains through binding to the N-terminal cytoplasmic domain of NRAMP1. Alternatively, the NRAMP1 molecule may possess quite different function(s) from NRAMP2. The same is known for the multi-drug resistance genes *MDR1* and *MDR2*. The *MDR1* gene encodes the multidrug transporter (P-glycoprotein), a multidrug efflux pump [44]. MDR1 is overexpressed in most multidrug-resistance cell lines, and confers multidrug resistance when transfected and overexpressed in otherwise drug-sensitive cells [45]. However, although MDR2 shows 78 % overall amino acid identity and has the same predicted domain organization as MDR1, MDR2 protein does not confer multidrug resistance and functions as a phosphatidylcholine flippase [46,47]. The NRAMP1 molecule may have different substrate specificity or quite different function(s) from NRAMP2.

We first simply supposed that the replacement of the N-terminal cytoplasmic domain of NRAMP1 with NRAMP2 counterpart would confer the divalent metal transport activity to this chimera. However, this replacement of NRAMP1 could not confer the function, and also the replacement of other domains could not do that. These results indicated that the sequences responsible for the functional differences between NRAMP1 and NRAMP2 are not located only in the N-terminal cytoplasmic domains, and also additional protein segments located elsewhere in NRAMP may determine these distinct functions. We then speculated that the diversity of modern mammalian NRAMPs may have initiated from the acquirement of the specific N-terminal cytoplasmic domains of each NRAMP molecule, and during evolution the NRAMP molecules may have changed in other segments endowing them with specific function(s). We are now making the mutations of NRAMP1 or NRAMP211 by the method of randomized PCR, and are going to investigate the divalent metal transport activity of those clones in *pdt1Δ* cells. These results will give us the chance to identify the protein segments located elsewhere in NRAMP1 which may determine the functional differences between NRAMP1 and NRAMP2.

We thank T. Yanagiya and A. Umetani, Fujirebio Inc., Japan for helping us to prepare the rabbit antiserum. We thank K. Ito, K. Doi, N. Tanaka and K. Fujita for their excellent technical assistance. We thank Dr H. Gunshin for a valuable discussion. We also thank Dr T. Nakazawa for critical reading of the manuscript. This work was partly supported by grants from the Ministry of Education, Science, Sports and Culture of Japan.

REFERENCES

1 Vidal, S. M., Malo, D., Vogan, K., Skamene, E. and Gros, P. (1993) Cell **73**, 469–485
2 Cellier, M., Prive, G., Belouchi, A., Kwan, T., Rodorigues, V., Chia, W. and Gros, P. (1995) Proc. Natl. Acad. Sci. U.S.A. **92**, 10089–10093
3 Cellier, M., Belouchi, A. and Gros, P. (1996) Trends Genet. **12**, 201–204
4 Barton, C. H., White, J. K., Roach, T. I. A. and Blackwell, J. M. (1994) J. Exp. Med. **179**, 1683–1687
5 Bairoch, A. (1991) Nucleic Acids Res. **19**, 2241–2245
6 Kishi, F. (1994) Biochem. Biophys. Res. Commun. **204**, 1074–1080
7 Kishi, F., Tanizawa, Y. and Nobumoto, M. (1996) Mol. Immunol. **33**, 265–268
8 Cellier, M., Govoni, G., Vidal, S., Kwan, T., Groulx, N., Liu, J., Sanchez, F., Skamene, E., Schurr, E. and Gros, P. (1994) J. Exp. Med. **180**, 1741–1752
9 Blackwell, J. M., Barton, C. H., White, J. K., Searle, S., Baker, A. M., Williams, H. and Shaw, M. A. (1995) Mol. Med. **1**, 194–205
10 Gruenheid, S., Pinner, E., Desjardins, M. and Gros, P. (1997) J. Exp. Med. **185**, 717–730
11 Atkinson, P. G. P., Blackwell, J. M. and Barton, C. H. (1997) Biochem. J. **325**, 779–786
12 Searle, S., Bright, N. A., Roach, T. I. A., Atkinson, P. G. P., Barton, C. H., Meloen, R. H. and Blackwell, J. M. (1998) J. Cell Sci. **111**, 2855–2866
13 Kishi, F., Yoshida, T. and Aiso, S. (1996) Mol. Immunol. **33**, 1241–1246
14 Tokuraku, K., Nakagawa, H., Kishi, F. and Kotani, S. (1998) FEBS Lett. **428**, 63–67
15 Gruenheid, S., Cellier, M., Vidal, S. and Gros, P. (1995) Genomics **25**, 514–525
16 Vidal, S., Belouchi, A.-M., Cellier, M., Beatty, B. and Gros, P. (1995) Mamm. Genome **6**, 224–230
17 Kishi, F. and Tabuchi, M. (1997) Mol. Immunol. **34**, 839–842
18 Gunshin, H., Mackenzie, B., Berger, U. V., Gunshin, Y., Romero, M. F., Boron, W. F., Nussberger, S., Gollan, J. L. and Hediger, M. A. (1997) Nature (London) **388**, 482–488
19 Fleming, M. D., Trenor, III, C., Su, M. A., Foernzler, D., Beier, D. R., Dietrich, W. F. and Andrews, N. C. (1997) Nature Genet. **16**, 383–386
20 Fleming, M. D., Romano, M. A., Su, M. A., Garrick, L. M., Garrick, M. D. and Andrews, N. C. (1998) Proc. Natl. Acad. Sci. U.S.A. **95**, 1148–1153
21 West, A. H., Clark, D. J., Martin, J., Neupert, W., Hartl, F. U. and Horwich, A. L. (1992) J. Biol. Chem. **267**, 24625–24633
22 Superk, F., Supekova, L., Nelson, H. and Nelson, N. (1996) Proc. Natl. Acad. Sci. U.S.A. **93**, 5105–5111
23 Liu, X. F., Superk, F., Nelson, N. and Culotta, V. C. (1997) J. Biol. Chem. **272**, 11763–11769
24 Pinner, E., Gruenheid, S., Raymond, M. and Gros, P. (1997) J. Biol. Chem. **272**, 28933–28938
25 Tabuchi, M., Iwaihara, O., Ohtani, Y., Ohuchi, N., Sakurai, J., Morita, T., Iwahara, S. and Takegawa, K. (1997) J. Bacteriol. **179**, 4179–4189
26 Moreno, S., Klar, A. and Nurse, P. (1991) Methods Enzymol. **194**, 795–823
27 Okazaki, K., Okazaki, K., Kume, K., Jinno, S., Tanaka, K. and Okayama, H. (1990) Nucleic Acids Res. **18**, 6485–6489
28 Tanaka, N., Ohuchi, N., Mukai, Y., Osaka, Y., Ohtani, Y., Tabuchi, M., Bhuiyan, M. S. A., Fukui, H., Harashima, S. and Takegawa, K. (1998) Biochem. Biophys. Res. Commun. **245**, 246–253
29 Kunkel, T. A. (1991) Methods Enzymol. **204**, 125–139
30 Kleid, D. G., Yansura, D., Samll, B., Dowbenko, D., Moore, M., Grubman, M. G., McKercher, P. D., Morgan, D. O., Robertoson, B. H. and Bachrach, H. L. (1981) Science **214**, 1125–1129
31 Chikashige, Y., Ding, D.-Q., Funabiki, H., Haraguchi, T., Mashiko, S., Yanagida, M. and Hiraoka, Y. (1994) Science **264**, 270–273
32 Vida, T. A. and Emr, S. D. (1995) J. Cell Biol. **128**, 779–792
33 McLeod, M., Stein, M. and Beach, D. (1987) EMBO J. **6**, 729–736
34 Kishi, F. and Tabuchi, M. (1998) Biochem. Biophys. Res. Commun. **251**, 775–783

35 Kishi, F. and Nobumoto, M. (1995) Immunol. Lett. **47**, 93–96
36 Shpetner, H. S. and Vallee, R. B. (1989) Cell **59**, 421–432
37 Obar, R. A., Collins, C. A., Hammarback, J. A., Shpetner, H. S. and Vallee, R. B. (1990) Nature (London) **347**, 256–261
38 Miki, H., Miura, K., Matuoka, K., Nakata, T., Hirokawa, N., Orita, S., Kaibuchi, K., Takai, Y. and Takenawa, T. (1994) J. Biol. Chem. **269**, 5489–5492
39 Grabs, D., Slepnev, V. I., Songyang, S. Z., David, C., Lynch, M., Cantley, L. C. and De Camilli, P. (1997) J. Biol. Chem. **272**, 13419–13425
40 Scaife, R., Gout, I., Waterfield, M. D. and Margolis, R. L. (1994) EMBO J. **13**, 2574–2582
41 Shpetner, H. S. and Vallee, R. B. (1992) Nature (London) **355**, 733–735
42 Herskovits, J. S., Shpetner, H. S., Burgess, C. C. and Vallee, R. B. (1993) Proc. Natl. Acad. Sci. U.S.A. **90**, 11468–11472
43 Barylko, B., Binns, D., Lin, K.-M., Atkinson, M. A. L., Jameson, D. M., Yin, H. L. and Alvanesi, J. P. (1998) J. Biol. Chem. **273**, 3791–3797
44 Gottesman, M. M. and Pastan, I. (1993) Annu. Rev. Biochem. **62**, 385–427
45 Ueda, K., Cardarelli, C., Gottesman, M. M. and Pastan, I. (1987) Proc. Natl. Acad. Sci. U.S.A. **84**, 3004–3008
46 Smit, J. J., Schinkel, A. H., Oude-Elferink, R. P., Groen, A. K., Wagenaar, E., van Deemter, L., Mol, C. A., Ottenhoff, R., van der Lugt, N. M., van Roon, M. A., et al. (1993) Cell **75**, 451–462
47 Ruetz, S. and Gros, P. (1994) Cell **77**, 1071–1081

Received 17 May 1999/20 July 1999; accepted 10 September 1999